The role of PALLD-STAT3 interaction in megakaryocyte differentiation and thrombocytopenia treatment

Guoming Li,[1*] Haojie Jiang,[1*] Lingbin Wang,[1] Tingting Liang,[1] Chen Ding,[1] Mina Yang,[1] Yingzhi Shen,[1] Min Xin,[2] Lin Zhang,[1] Jing Dai,[2] Xueqing Sun,[1] Xuejiao Chen,[3] Junling Liu[1,4] and Yanyan Xu[1]

[1]Department of Biochemistry and Molecular Cell Biology, Key Laboratory of Cell Differentiation and Apoptosis of Chinese Ministry of Education, Shanghai Jiao Tong University School of Medicine, Shanghai; [2]Department of Laboratory Medicine, Ruijin Hospital, Shanghai Jiao Tong University School of Medicine, Shanghai; [3]School of Basic Medicine, Hubei University of Arts and Science, Xiangyang, Hubei Province and [4]Shanghai Synvida Biotechnology Co., Ltd., Shanghai, China

**GL and HJ contributed equally as first authors.*

Correspondence: X. Chen
ruipiaoc@163.com

J. Liu
liujl@shsmu.edu.cn

Y. Xu
xuyanyan901@163.com

Received: February 7, 2024.
Accepted: May 21, 2024.
Early view: May 30, 2024.

https://doi.org/10.3324/haematol.2024.285242

Abstract

Impaired differentiation of megakaryocytes constitutes the principal etiology of thrombocytopenia. The signal transducer and activator of transcription 3 (STAT3) is a crucial transcription factor in regulating megakaryocyte differentiation, however the precise mechanism of its activation remains unclear. PALLD, an actin-associated protein, has been increasingly recognized for its essential functions in multiple biological processes. This study revealed that megakaryocyte/platelet-specific knockout of *Palld* in mice exhibited thrombocytopenia due to diminished platelet biogenesis. In megakaryocytes, PALLD deficiency led to impaired proplatelet formation and polyploidization, ultimately weakening their differentiation for platelet production. Mechanistic studies demonstrated that PALLD bound to STAT3 and interacted with its DNA-binding domain and Src homology 2 domain via immunoglobulin domain 3. Moreover, the absence of PALLD attenuated STAT3 Y705 phosphorylation and impeded STAT3 nuclear translocation. Based on the PALLD-STAT3 binding sequence, we designed a peptide C-P3, which can facilitate megakaryocyte differentiation and accelerate platelet production *in vivo*. In conclusion, this study highlights the pivotal role of PALLD in megakaryocyte differentiation and proposes a novel approach for treating thrombocytopenia by targeting the PALLD-STAT3 interaction.

Introduction

Thrombocytopenia presents clinical concern due to its high incidence and potential for severe complications. It is defined by platelet counts falling below 0.15×10^{12}/L, resulting in significant spontaneous bleeding and subcutaneous purpura.[1,2] Notably, when the platelet counts fall below 0.02×10^{12}/L, patients will face a substantial risk of severe hemorrhagic events, such as traumatic intracranial bleeding and gastrointestinal hemorrhage.[3] Thrombocytopenia has a variety of causes. Impaired differentiation of megakaryocytes, leading to a reduction in platelet counts, constitutes the principal etiology of thrombocytopenia.

Megakaryocytes are derived from hematopoietic stem cells and predominantly reside within the bone marrow.[4,5] During thrombocytopoiesis, megakaryocytes differentiate through a series of tightly regulated complex processes, including endomitosis, membrane system invagination, and proplatelet formation (PPF).[6,7] Research in megakaryocyte differentiation enhances our understanding of platelet production, which is critical for managing thrombocytopenia. The TPO/Mpl/JAK2/STAT3 pathway is the principal signaling pathway responsible for regulating megakaryocyte differentiation and platelet production.[8,9] When thrombopoietin (TPO) binds and activates the myeloproliferative leukemia protein (MPL), the receptor-associated Janus kinase 2 (JAK2) is subsequently phosphorylated, recruiting and phosphorylating the signal transducer and activator of transcription 3 (STAT3).[10-12] STAT3 enters the nucleus and binds to the promoter regions of specific genes, such as *MYC* and Zinc Finger Protein 460 (*ZNF460*), through the DNA-binding domain (DBD), thus regulating the expression

of such genes.[13,14] Given STAT3's central role in executing the cellular responses initiated by the pathway, targeting STAT3 may be a key to understanding megakaryocyte differentiation.

PALLD, belonging to the cytoskeletal immunoglobulin domain-containing family, exhibits ubiquitous expression in mammals and localizes to various actin-rich subcellular structures, including stress fibers and focal adhesions.[15-17] Studies recently have shown the critical role of PALLD in various physiological and pathological processes. During the early stages of smooth muscle cell (SMC) differentiation, PALLD interacts with the CArG element within the genome to regulate the expression of smooth muscle actin (SMA) and SM22, thus promoting precursor SMC differentiation.[18] PALLD can also promote cancer stem cell-like properties and tumorigenicity by activating the Wnt/β-catenin signaling pathway.[19] Our previous study reported that PALLD exhibited abundant expression in platelets and was involved in the activation of platelets.[20] This prompted us to consider whether PALLD had an earlier role in megakaryocytes and potentially in platelet biogenesis.

This study found that the absence of PALLD significantly inhibited megakaryocyte differentiation, leading to thrombocytopenia. PALLD interacts with the SH2 domain and DBD of STAT3 to sustain STAT3 function during megakaryocyte differentiation. By exploiting the binding sequence of PALLD and STAT3, we have developed peptide C-P3 that can enhance STAT3 activation and promote thrombopoiesis *in vivo*. These findings help to reveal the molecular mechanisms underlying megakaryocyte differentiation and provide a promising target for the intervention of thrombocytopenia.

Methods

Mice, antibodies, reagents and more methods

Detailed descriptions of antibodies, reagents, mice and other methods are included in the *Online Supplementary Appendix*.

Platelet preparation

Platelets were prepared as described before.[21] Briefly, whole blood (including 1 U/mL apyrase and 0.1 μg/mL PGE1) was centrifugated at 200xg for 10 minutes (min) to obtain platelet-rich plasma (PRP). PRP (including 5 mM EDTA) was centrifugated at 800xg for 10 min to obtain washed platelets. Human platelet preparation and related experiments were approved by the Research Ethics Committee of Shanghai Jiao Tong University College of Basic Medical Sciences.

Flow cytometry and flow sorting

Cells from blood and bone marrow were separated and resuspended in FACS buffer. For reticulated platelets analysis, cells were stained with thiazole orange for 60 min. For apoptotic platelet analysis, cells were stained with Annexin V for 10 min. Both samples were detected on CytoFLEX (Beckman Coulter). For megakaryocyte sorting, cells were stained with anti-CD41 and anti-CD42b antibodies for 30 min, and sorted on FACS Aria II (BD Biosciences).

Platelet lifespan assay

Mice were injected with Sulfo-NHS-LC-Biotin via the tail vein. Platelets from orbital blood were separated and stained with streptavidin. Flow cytometry was used to measure the mean fluorescence intensity of streptavidin in platelets.

Platelet regeneration assay

Mice were injected with anti-CD42b antibody (Emfret) via the tail vein. Platelets from orbital blood were quantified using the XN-1000V automatic modular animal blood and body fluid analyzer (Sysmex).

Megakaryocyte induction and differentiation

Megakaryocytes were prepared as described before.[22] Briefly, fetal livers were obtained from 13.5-day pregnant mice and cultured in Dulbecco's modified medium containing 10% fetal bovine serum, 1% penicillin/streptomycin stock solution (10,000 U/mL), and 25 IU/mL recombinant human TPO (3SBIO) for 4 days. Purified megakaryocytes were separated by 3% bovine serum albumin and 1.5% bovine serum albumin.

Megakaryocyte proplatelet forming and ploidy assay

Fetal liver-derived megakaryocytes were cultured on slides coated with fibrinogen (Sigma) for differentiation. Then they were fixed and stained with anti-α-tubulin antibody, imaged using TCS SP8 X (Leica) or N-SIM (Nikon). For the ploidy assay, megakaryocytes were stained with anti-CD41 antibody and fixed overnight. Then they were incubated with 50 μg/mL propidium iodide, 100 μg/mL RNase A, and 0.2 % Triton X-100 for 30 min. Polyploidy was analyzed using flow cytometry.

Enzyme-linked immunosorbent assay

HEK293T cells were transfected with pcDNA3.1-Flag or Flag-STAT3 plasmids for 48 hours. Total protein was collected using lysis buffer and added to wells coated with PALLD peptides. Each well was incubated with anti-Flag antibody (Sigma) for 1 hour at room temperature, followed by horseradish peroxidase (HRP)-conjugated secondary antibody (Jackson ImmunoResearch Laboratories); 2 M H_2SO_4 was used to terminate the color change. The absorption at 450 nm was measured.

Data analysis

Data analysis for the experiment was conducted using GraphPad Prism 9 software. A significance level of $P \leq 0.05$ was considered to determine statistically significant variations among the values.

Results

PALLD deficiency diminishes platelet production in mice

In order to investigate the impact of PALLD on platelets and megakaryocytes, we established megakaryocyte/platelet-specific PALLD knockout mice (*pf4-Cre*$^{+}$ *Palld*$^{f/f}$, *Palld*$^{-/-}$).[23,24] As expected, PALLD protein levels were decreased in *Palld*$^{-/-}$ platelets but remained unchanged in other hemocytes (Figure 1A). Peripheral blood cell analysis revealed significantly reduced platelet counts in the *Palld*$^{-/-}$ mice ($0.45\pm0.02\times10^{12}$ platelets/L), compared to the *Palld*$^{f/f}$ mice ($0.94\pm0.05\times10^{12}$ platelets/L), while red and white blood cell counts, mean platelet volume (MPV) and platelet distribution width (PDW), dense and α granules of platelets remained unaltered, collectively indicating thrombocytopenia in *Palld*$^{-/-}$ mice (Figure 1B; *Online Supplementary Figure S1A, B*).

Impaired platelet production or excessive platelet clearance can lead to thrombocytopenia.[5,25] In peripheral blood, the proportion of newly generated platelets (Figure 1C; *Online Supplementary Figure S1C*) of *Palld*$^{-/-}$ mice (3.50±0.11%) was significantly lower than that of *Palld*$^{f/f}$ mice (5.74±0.13%), and the proportion of apoptotic platelets remained unchanged (Figure 1D; *Online Supplementary Figure S1D*). We further measured platelet regeneration and clearance rates *in vivo*. Anti-CD42b monoclonal antibody was used to deplete platelets, and platelet counts measured at different time

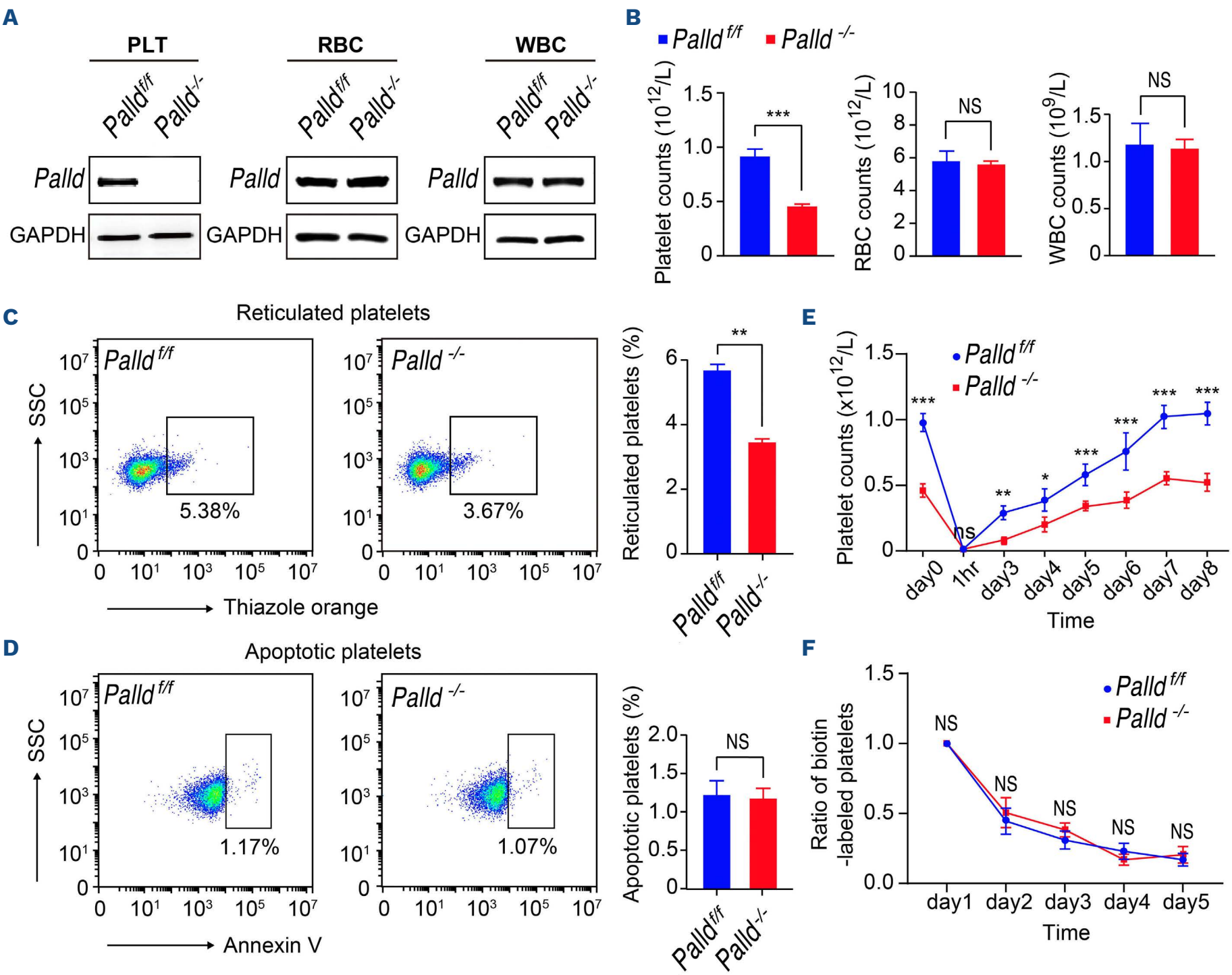

Figure 1. Impaired platelet biogenesis leads to thrombocytopenia in *Palld*$^{-/-}$ mice. (A) Western blot analysis of PALLD expression in platelets, red blood cells (RBC) and white blood cells (WBC) of *Palld*$^{f/f}$ and *Palld*$^{-/-}$ mice. (B) Platelet, RBC and WBC counts in *Palld*$^{f/f}$ and *Palld*$^{-/-}$ mice (N=7; ***P<0.001; NS: not significant). (C) Representative gating strategy of thiazole orange-stained cells and percentage of reticulated platelets in *Palld*$^{f/f}$ and *Palld*$^{-/-}$ mice (N=4; **P<0.01). (D) Representative gating strategy of annexin V-stained cells and percentage of apoptotic platelets in *Palld*$^{f/f}$ and *Palld*$^{-/-}$ mice (N=4). (E) Platelet counts at different time points after intravenous tail injection of anti-CD42b antibody (2 μg/g) (N=4; *P<0.05, **P<0.01, ***P<0.001). (F) Biotin-labeled platelets in mice at different time points after tail intravenous injection of Sulfo-NHS-LC-Biotin (N=4).

points showed that platelet regeneration was diminished in *Palld*$^{-/-}$ mice compared to *Palld*$^{f/f}$ mice (Figure 1E). After intravenous tail injection of Sulfo-NHS-LC-Biotin, the proportions of biotin-labeled platelets at different time points indicated similar rates of platelet clearance between *Palld*$^{f/f}$ mice and *Palld*$^{-/-}$ mice (Figure 1F). These data suggested that PALLD deficiency impaired platelet production, resulting in thrombocytopenia in mice.

PALLD deficiency impairs megakaryocyte differentiation

In order to explore the reason for reduced platelet biogenesis in *Palld*$^{-/-}$ mice, we evaluated the differentiation ability and number of megakaryocytes. Under TPO stimulation, hematopoietic stem cells in the fetal liver differentiate into megakaryocytes and subsequently mature, extending proplatelets.[26,27] We found that fetal liver-derived *Palld*$^{-/-}$ megakaryocytes generated fewer proplatelets than *Palld*$^{-/-}$ megakaryocytes at 6 and 8 hours, with decreased number of proplatelet tips, while the F-actin morphology and tip diameter remained relatively unchanged (Figure 2A-C; *Online Supplementary Figure S2A-C*). The unaltered tip diameter in *Palld*$^{-/-}$ megakaryocytes is consistent with our observations of unchanged MPV and PDW (*Online Supplementary Figure S1A*). During megakaryocyte differentiation, endomitosis results in accumulated DNA content and the formation of high ploidy in megakaryocytes. *Palld*$^{-/-}$ megakaryocytes derived from the fetal liver or bone marrow showed a higher proportion of normal ploidy (≤ 4N) and a lower ratio of hyperploid (≥ 8N) (Figure 2D-E). From these data, PALLD deficiency impaired megakaryocyte proplatelet formation and polyploidization. Immunohistochemistry analysis of major thrombopoiesis organs (bone marrow and spleen) in mice revealed that PALLD deficiency had no effect on the number of megakaryocytes (Figure 3A, B).[28,29] CFU-MK assay indicated that PALLD deficiency did not impact the ability of bone marrow and fetal liver-derived cells to form colonies (Figure 3C).[30]

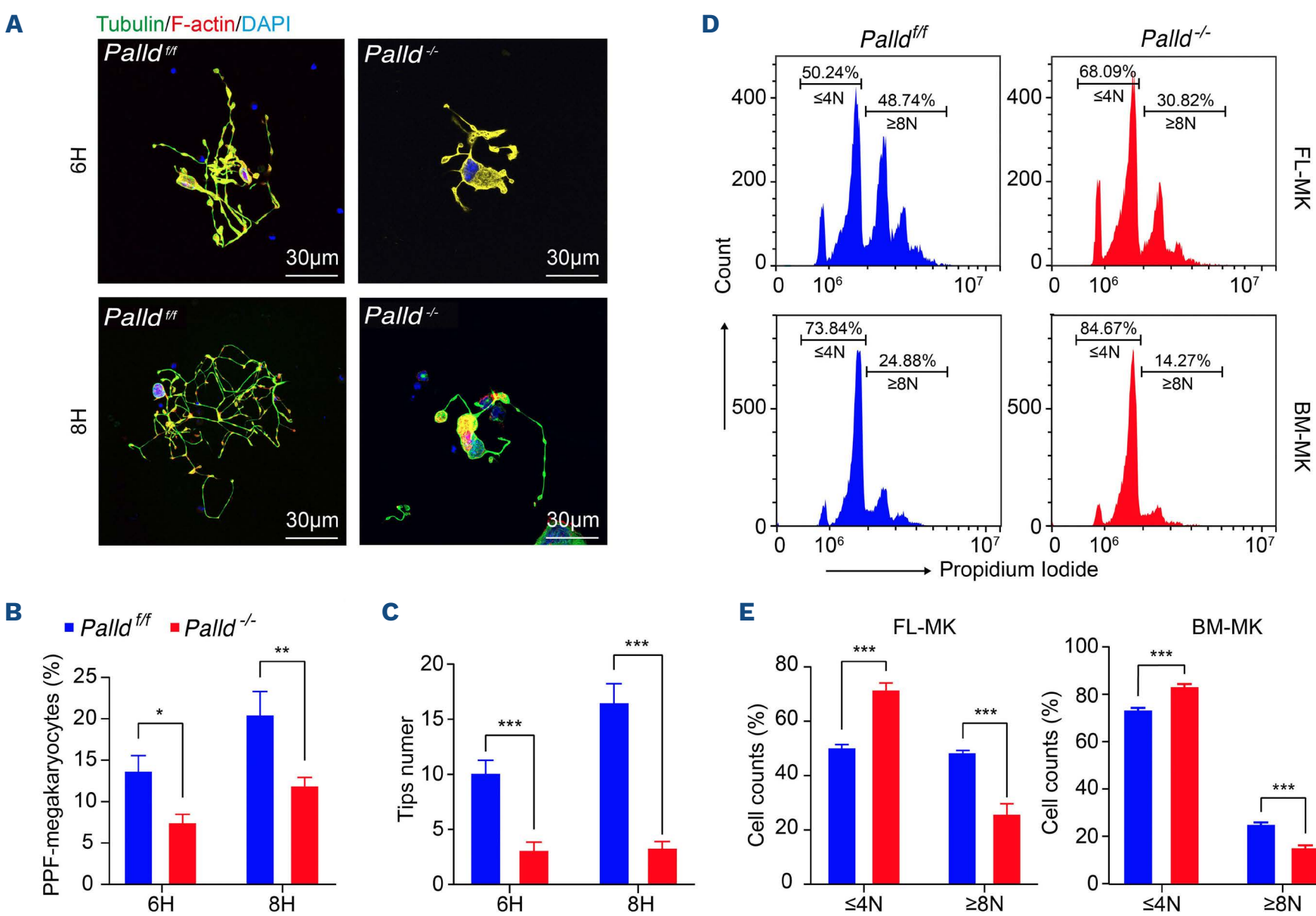

Figure 2. PALLD deficiency impairs megakaryocyte proplatelet formation and polyploidization. (A) Immunofluorescence (IF) images of proplatelet-forming (PPF) megakaryocytes derived from the fetal liver (FL-MK) of *Palld*$^{f/f}$ and *Palld*$^{-/-}$ mice, stained with α-tubulin (Alexa Fluor 488), F-actin (Rhodamine). The scale bars represent 30 μm. (B) Quantitative analysis of the ratio of PPF-megakaryocytes to total megakaryocytes (6 hours [6H], N=5; **P*<0.05; (8 hours [8H], N=5; ***P*<0.01). (C) Number of proplatelet tips generated by *Palld*$^{f/f}$ and *Palld*$^{-/-}$ megakaryocytes (6H, N=5; ****P*<0.001; 8H, N=5). (D) Representative gating strategy for propidium iodide staining of FL-MK and megakaryocytes from bone marrow (BM-MK) in *Palld*$^{f/f}$ and *Palld*$^{-/-}$ mice. (E) Quantitative analysis of the polyploidy ratio in megakaryocytes from fetal liver and bone marrow of *Palld*$^{f/f}$ and *Palld*$^{-/-}$ mice (N=4, ****P*<0.001).

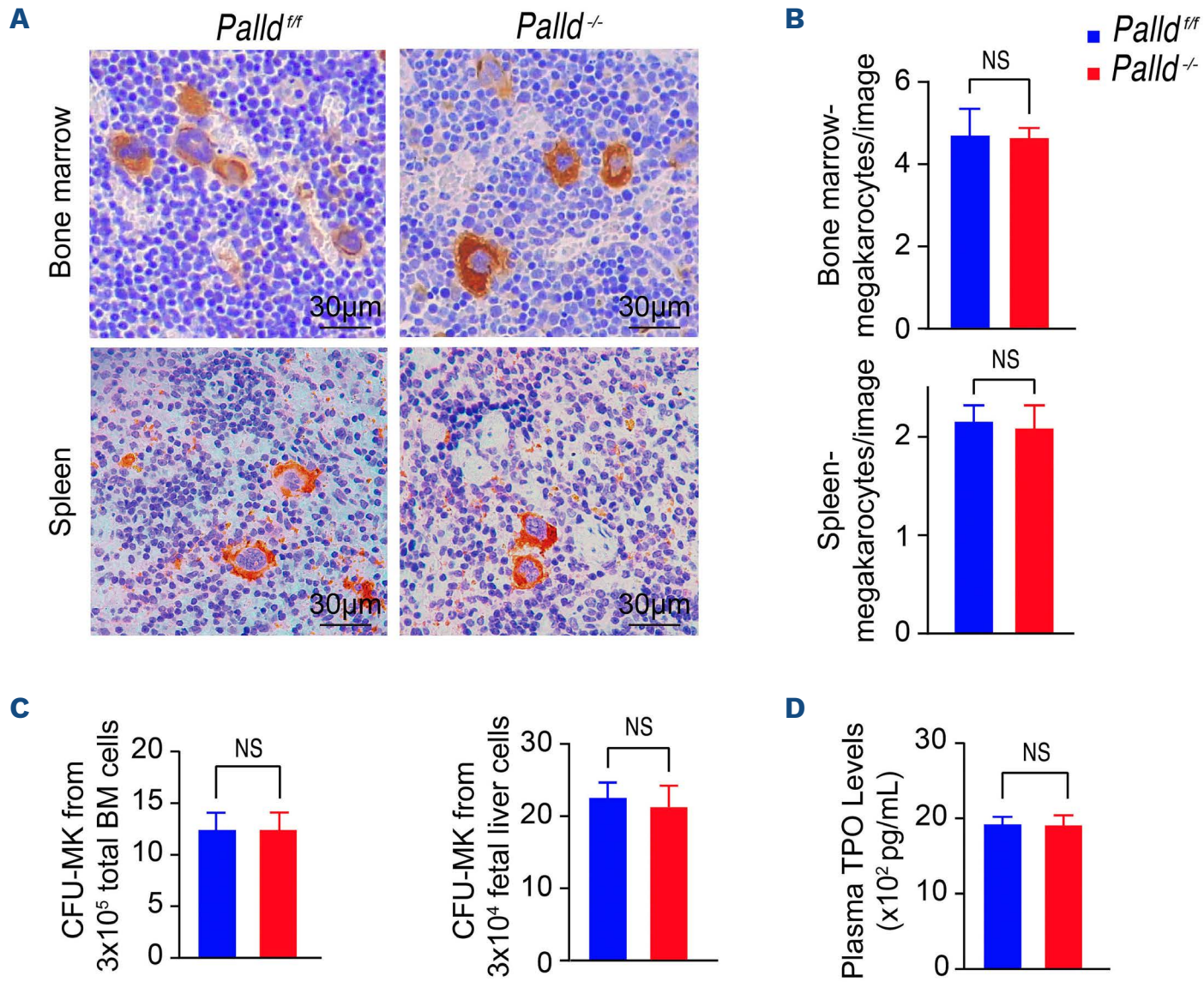

Figure 3. PALLD deficiency has no effect on megakaryocyte number and colony formation. (A) Immunohistochemistry images of megakaryocytes in the femur and spleen of *Palld*$^{f/f}$ and *Palld*$^{-/-}$ mice. The scale bars represent 30 μm. (B) Quantitative analysis of megakaryocyte counts in the femur (N=7) and spleen (N=15) sections from *Palld*$^{f/f}$ and *Palld*$^{-/-}$ mice. (C) Colony-forming unit megakaryocyte (CFU-MK) assay of bone marrow (BM) and fetal liver-derived cells from *Palld*$^{f/f}$ and *Palld*$^{-/-}$ mice (N=5). (D) Plasma thrombopoietin (TPO) levels in *Palld*$^{f/f}$ and *Palld*$^{-/-}$ mice (N=7).

The plasma TPO remained at a similar level in *Palld*$^{f/f}$ and *Palld*$^{-/-}$ mice (Figure 3D). All these data show that PALLD deficiency impaired megakaryocyte differentiation, leading to thrombocytopenia in mice.

PALLD interacts with STAT3 and sustains STAT3 activation in megakaryocyte differentiation

In order to understand the molecular mechanism of PALLD's impact on megakaryocyte differentiation, we collected total RNA and PALLD co-immunoprecipitation (Co-IP) proteins from bone marrow-derived megakaryocytes of *Palld*$^{f/f}$ and *Palld*$^{-/-}$ mice, and performed next-generation RNA sequncing and liquid chromatography-mass spectrometry (LC-MS) respectively (Figure 4A).

Differentially expressed genes (P<0.05; log fold change [$\log_2$FC] >1.0) were clustered, revealing 73 upregulated and 63 downregulated genes in *Palld*$^{-/-}$ megakaryocytes compared to *Palld*$^{f/f}$ megakaryocytes (Figure 4B; *Online Supplementary Figure S2D*; *Online Supplementary Tables S1, S2*). Among these, the JAK-STAT pathway showed significant enrichment by gene ontology (GO) analysis (Figure 4C; *Online Supplementary Table S3*). Based on the mass spectrometry results, we found that PALLD interacted with STAT3. Co-IP experiments in human platelets or HEK293T cells also confirmed that PALLD bound to STAT3 (Figure 4D, E).

STAT3 is a crucial transcription factor in megakaryocyte differentiation, which can be activated by the TPO/Mpl/JAK2 pathway.[22,31] After treating platelets and megakaryocytes with TPO, we found reduced phosphorylation level of STAT3 Y705 in *Palld*$^{-/-}$ platelets and megakaryocytes (Figure 4F; *Online Supplementary Figure S2E*). In PPF experiments, nuclear localization of STAT3 decreased in *Palld*$^{-/-}$ megakaryocytes derived from the fetal liver compared to that of *Palld*$^{f/f}$ (Figure 4G, H). These findings suggest that PALLD participates in preserving TPO-stimulated STAT3 activation in platelets and megakaryocytes.

PALLD interacts with the DNA-binding domain and Src homology 2 domain of STAT3 and co-localizes with STAT3 in both the nucleus and cytoplasm

Among the various isoforms of PALLD, the 90 kDa isoform

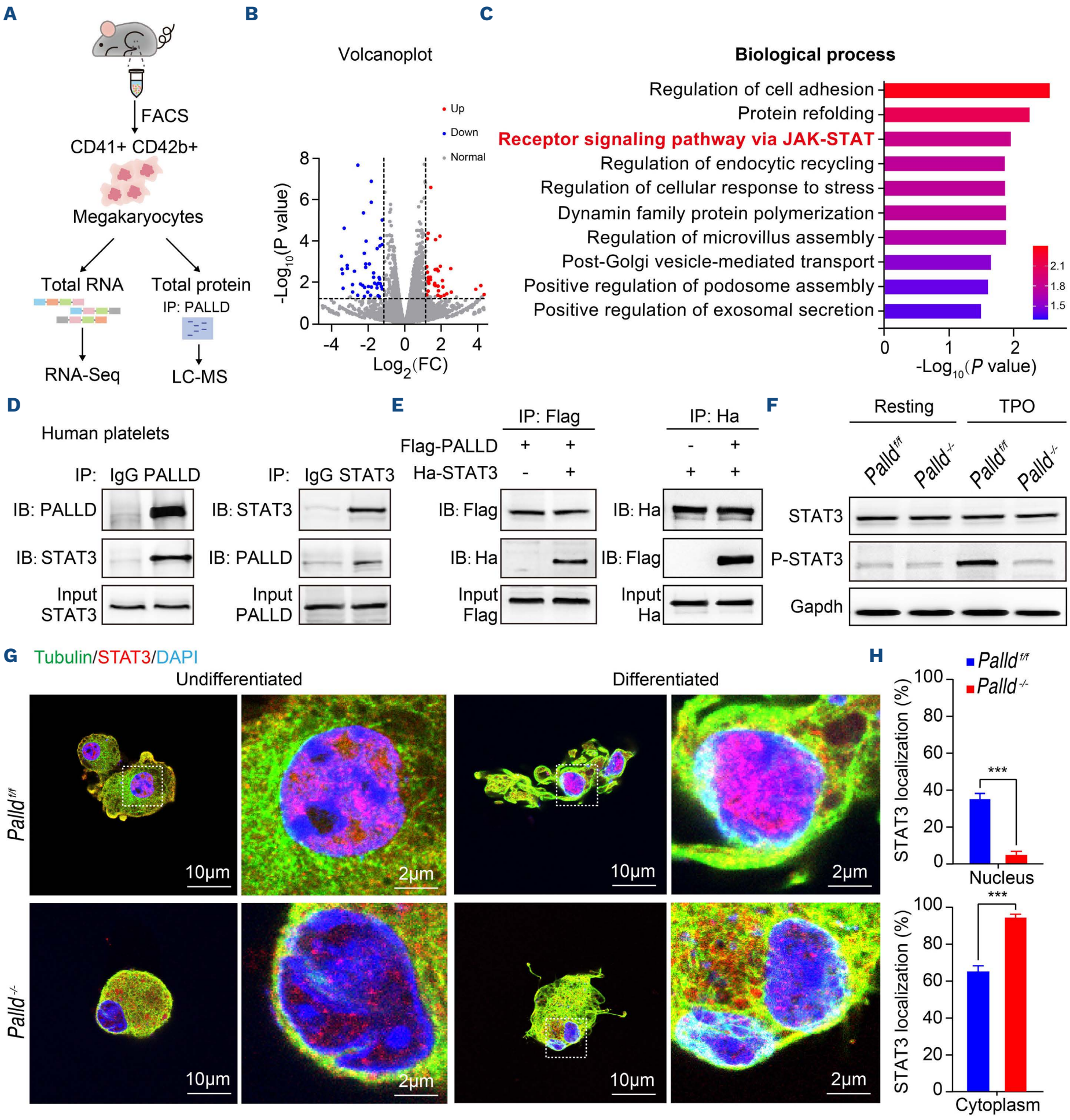

Figure 4. PALLD maintains thrombopoietin-induced STAT3 activation in platelets and megakaryocytes. (A) Schematic diagram of RNA sequencing (RNA-seq) and liquid chromatography-mass spectrometry (LC-MS) of bone marrow-derived megakaryocytes. (B) Volcano plot of global gene expression profiles in bone marrow megakaryocytes from *Palld*$^{f/f}$ and *Palld*$^{-/-}$ mice. Kolmogorov-Smirnov (K-S) test was used for testing the correlation. Downregulated genes are shown in blue and upregulated genes are in red. (C) Gene ontology (GO) enrichment analysis of functional categories among down-regulated genes in the *Palld*$^{-/-}$ megakaryocytes. The bar chart represents the enriched GO terms, and the color indicates the significance level. (D) Co-immunoprecipitation (Co-IP) of human platelet lysates using anti-PALLD and anti-STAT3 antibodies. (E) Co-IP of lysates from HEK293T cells transfected with Flag-STAT3 and Ha-PALLD.(F) Western blot of the phosphorylation level of STAT3 Y705 in platelets treated with 25 IU/mL thrombopoietin. (G-H) IF images of undifferentiated and differentiated megakaryocytes derived from the fetal livers of *Palld*$^{f/f}$ and *Palld*$^{-/-}$ mice. Stained for α-tubulin (Alexa Fluor 488) and STAT3 (Rhodamine). Statistical results of STAT3 localization are presented (N=5; ***P<0.001). The scale bars represent 10 μm or 2 μm.

was the most abundant in platelets, while others, such as the 200 kDa isoform or 140 kDa isoform, were nearly unexpressed (*Online Supplementary Figure S2F*).[32] This led us to focus our research on the 90 kDa PALLD isoform.

In order to explore the precise domains responsible for the PALLD-STAT3 interaction, we designed truncated forms of both proteins based on their fundamental structures and expression stability. The results of Co-IP experiments demonstrated that PALLD interacted with the DNA-binding domain (DBD) and Src homology 2 (SH2) domain of STAT3, and STAT3 interacted with the immunoglobulin domain 3 (Ig3) of PALLD (Figure 5A-C). Using the protein-protein

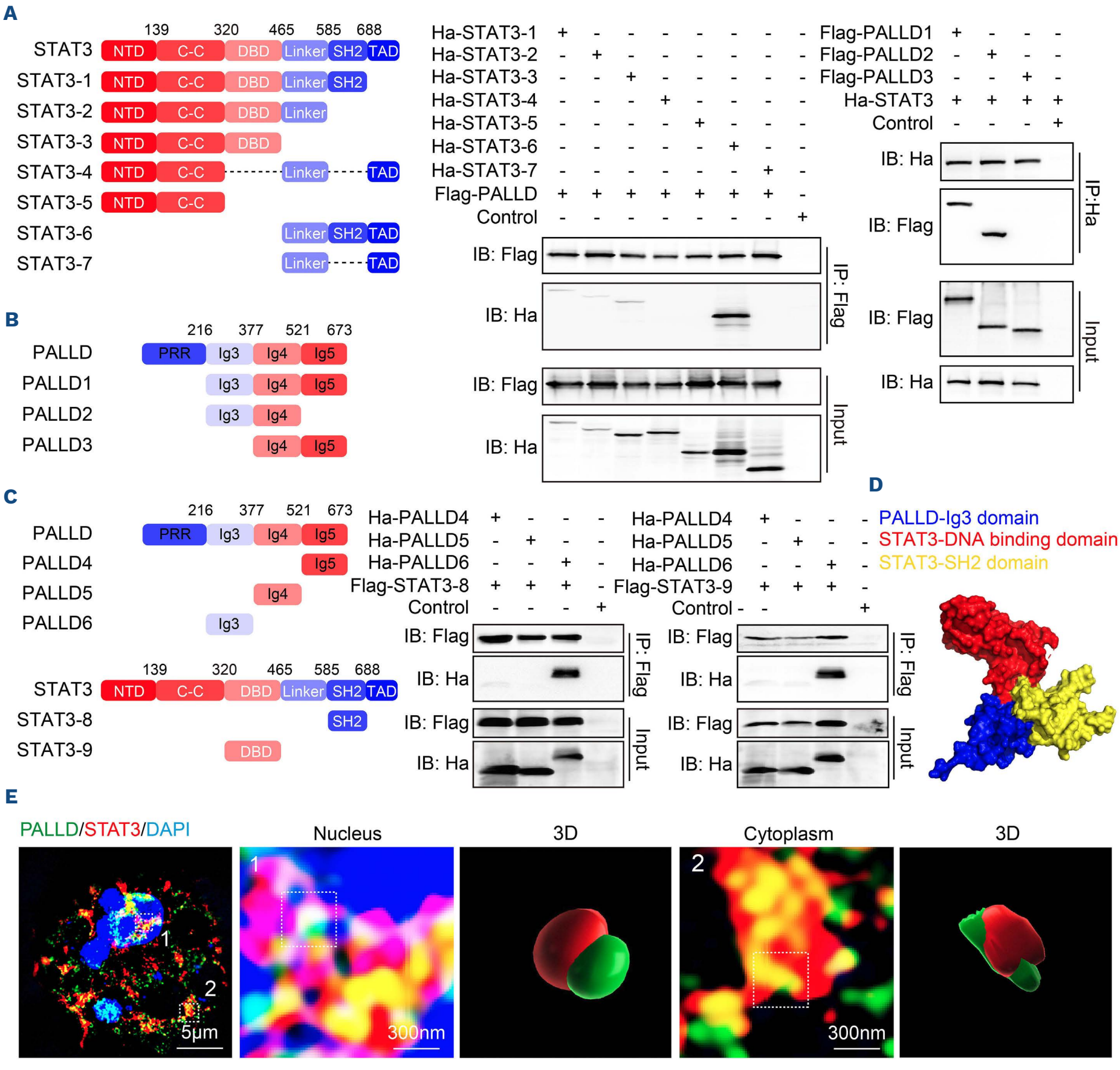

Figure 5. The Ig3 domain of PALLD binds to the DNA-binding domain and Src homology 2 domain of STAT3 in both the nucleus and cytoplasm. (A-C) Co-immunoprecipitation (Co-IP) of lysates from HEK293T cells transfected with the truncated forms of STAT3 or PALLD. (D) Surface-binding model of PALLD's immunglobulin 3 (Ig3) domain with STAT3's DNA-binding domain (DBD) and Src homology 2 (SH2) domain. (E) Immunofluorescence (IF) images of endogenous PALLD (Alexa Fluor 488) and STAT3 (Rhodamine) in megakaryocytes derived from fetal liver. The 3D-volume rendering of PALLD and STAT3 signals was performed using Imaris software. The scale bars represent 5 μm or 300 nm. PRR: proline rich region; NTD: N-terminal domain; C-C: coiled-coil domain; TAD: transactivation domain.

docking model, we predicted a surface binding model for the interaction between PALLD's Ig3 domain, STAT3's DBD and SH2 domain (Figure 5D).

Under a super-resolution structured illumination microscope (SIM), PALLD co-localized with STAT3 in the cytoplasm and nucleus (Figure 5E). Co-IP results also confirmed PALLD-STAT3 interaction in the cytoplasm and nucleus (*Online Supplementary Figure S3C, D*). Additionally, PALLD and STAT3 showed diminished localization in the nucleus when treated with nuclear import inhibitor Ivermectin (Iver) and accumulated in the nucleus when treated with nuclear export inhibitor Leptomycin B (LMB) (*Online Supplementary Figure S3A, B*).[33-35] All data showed that PALLD co-localized with STAT3 in both the nucleus and cytoplasm.

Most proteins located at the nucleus in eukaryotic cells possess NLS that can facilitate protein transport through the nuclear pore complexes (NPC) into the nucleus.[36,37] We found that PALLD co-localized with NPC, and verified that the KPKK or PKKV sequence may serve as the NLS for PALLD (*Online Supplementary Figure S3E-G*). Furthermore, through chromatin immunoprecipitation (Ch-IP) and utilizing the STAT3-binding promoter sequence as primers (*Online Supplementary Figure S3H*), PALLD was found to interact with the STAT3 transcription complex and may act as a transcription co-factor of STAT3.[13,14]

Peptide C-P3 promotes megakaryocyte differentiation and platelet production

In order to further clarify the specific binding sequence between PALLD and STAT3, we divided the Ig3 domain of PALLD into seven shorter sequences (1-30, 31-60, 61-74, 75-100, 101-118, 119-145, and 146-162), each comprising 30 or fewer amino acids (Figure 6A). Enzyme-linked immonosorbant assay (ELISA) analysis showed notable interaction between peptide 75-100 and STAT3. Then, we subdivided peptide 75-100 into four shorter sequences (P1, P2, P3, P4) and found that peptide P3 exhibited distinct and specific binding to STAT3 (Figure 6B). P3 weakened the binding of PALLD to the DBD but strengthened the binding to the SH2 domain (Figure 6C). Furthermore, in the protein-protein docking model, P3 probably provided the optimal spatial configuration for the PALLD-STAT3 interaction (Figure 6D). Cell-penetrating peptides (CPP) are short peptides that facilitate the entry of biomacromolecules into cells through endocytosis or direct penetration of the cell membrane. In order to explore the cellular function of P3, we designed peptide C-P3 by fusing a kind of CPP, TAT (GRKKRRQRRR) derived from HIV, to the N terminus of P3 (Figure 7A).[38] IF images showed that C-P3 was successfully internalized and localized in megakaryocytes and platelets (Figure 7B; *Online Supplementary Figure S4A*). In platelets, C-P3 promoted the phosphorylation levels of STAT3 Y705 but had no effect on *Palld*$^{-/-}$ platelets (Figure 7C). In PPF experiments, C-P3 promoted megakaryocytes extend more and longer proplatelet branches as the concentration increased, culminating in forming a complex network structure (Figure 7D-E; *Online Supplementary Figure S4D*).

In order to further explore the function of C-P3 *in vivo*, this peptide was injected into the bone marrow of mice. Images and flow cytometry analysis further confirmed the penetration of peptide C-P3 (*Online Supplementary Figure S4B, C*). Moreover, C-P3 accelerated the rate of platelet regeneration, resulting in a quicker restoration of platelet levels to the normal range (Figure 7F). These findings provide evidence that C-P3 can activate STAT3 and promote megakaryocyte differentiation and platelet production (Figure 7G), providing a potential implication for the clinical treatment of thrombocytopenia.

Discussion

In this study, we found that mice lacking PALLD exhibited thrombocytopenia with decreased platelet production and poor PPF formation, indicating the role of PALLD in megakaryocyte differentiation. PALLD binds to STAT3 and sustains activation of STAT3 during megakaryocyte differentiation. Targeting the PALLD-STAT3 interaction may provide a promising target for the intervention of thrombocytopenia.

PALLD was initially characterized independently by two research groups,[16,17] as a molecular scaffold that regulates the cytoskeleton network. Previous studies have shown that PALLD binds to actin via the Ig3 domain and is localized in various actin-rich subcellular structures, including stress fibers, focal adhesions and Z disks.[15,39] Recent studies have reported novel roles of PALLD in cell adhesion and motility, contributing to the invasive motility of cancer cells.[40-42] Our former research also suggested that PALLD was involved in platelet activation and arterial thrombosis.[20] This study identified PALLD's role in megakaryocyte differentiation through interacting with STAT3, proposing and elaborating new mechanisms and functions of PALLD.

The TPO/Mpl/JAK2/STAT3 signaling pathway is the major signaling pathway to regulate megakaryocyte differentiation and platelet biogenesis. Once activated, STAT3 is phosphorylated and enters the nucleus to induce transcription of differentiation-related genes.[22,31] PALLD maintains TPO-induced STAT3 activation in platelets and megakaryocytes. When PALLD deficiency is present, reduced STAT3 activation probably affects the expression of several downstream genes, ultimately leading to impaired megakaryocyte differentiation. For example, *Fscn1*, a gene involved in actin cytoskeleton dynamics and transcriptionally regulated by STAT3, is significantly downregulated in *Palld*$^{-/-}$ megakaryocytes, and its reduced expression has been reported to be associated with decreased proplatelet formation.[43,44] The downstream molecular mechanism impacted by the PALLD-STAT3 interaction still needs further investigation. As a pivotal transcription factor, STAT3 regulates several

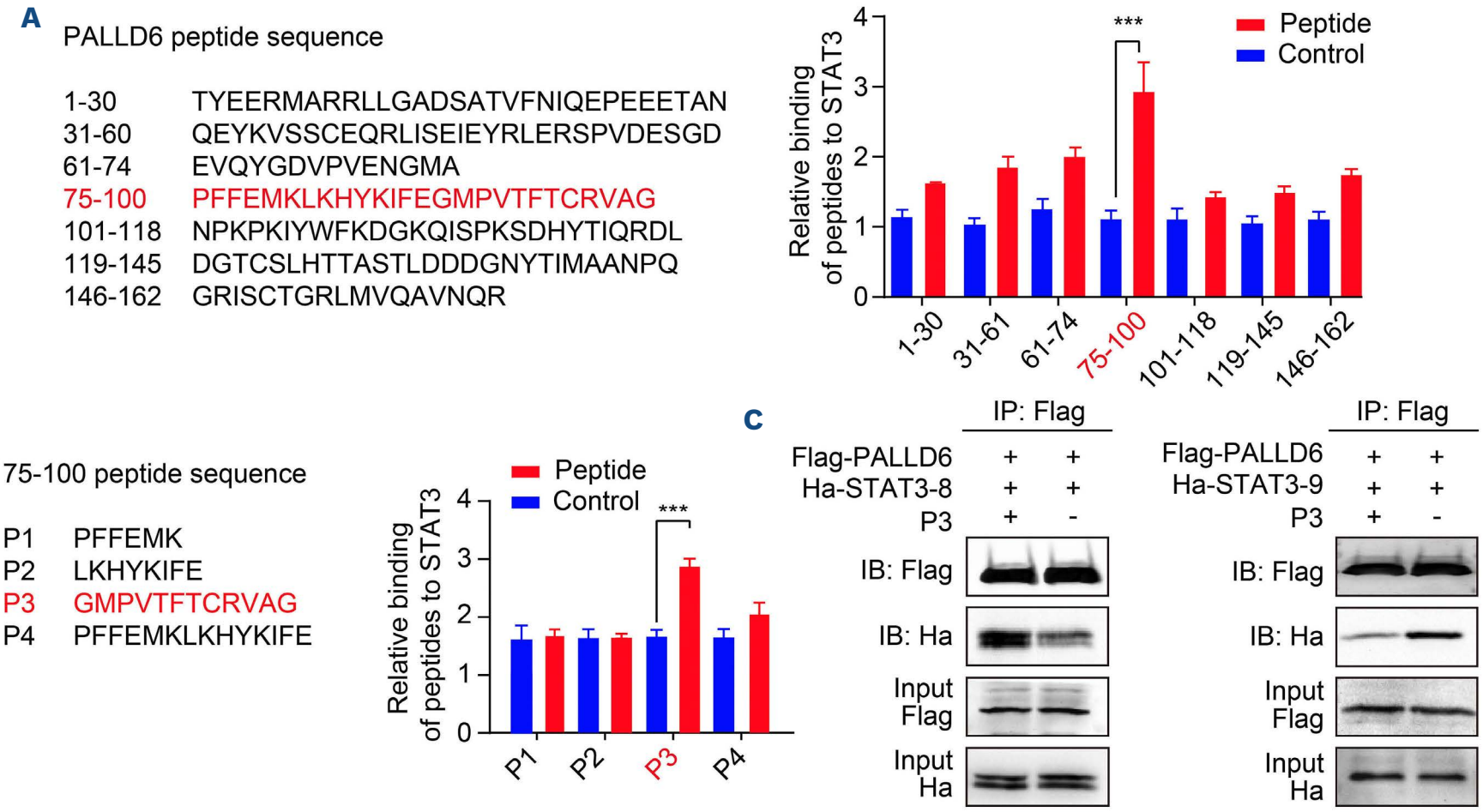

Figure 6. Peptide P3 impacts the interaction between PALLD and STAT3. (A) Binding affinity of 7 PALLD6 peptides to STAT3 detected by enzyme-linked immunosorbent assay (ELISA). Sequence and statistical analysis from 4 independent experiments are shown (***P<0.001). (B) Binding affinity of 4 75-100 peptides to STAT3 detected by ELISA. Sequence and statistical analysis of 4 independent experiments is shown (***P<0.001). (C) Co-immunoprecipitation (Co-IP) of lysates from HEK293T cells transfected with Flag-PALLD6 and either Ha-STAT3-8 or Ha-STAT3-9, with or without P3. (D) The binding model of PALLD's immunglobulin 3 (Ig3) domain interacting with STAT3's DNA-binding domain (DBD) and Src homology 2 (SH2) domain.

genes in hematopoietic stem and progenitor cells, affecting their function and differentiation.[45] Our study found that PALLD enters the nucleus with nuclear localization signals, co-localizes with STAT3 in the nucleus, and may act as a transcription co-factor. However, elucidating the precise mechanism of PALLD in STAT3-mediated transcription needs further in-depth exploration.

Beyond megakaryocyte differentiation, the constitutive activation of STAT3 is related to the occurrence of multiple tumors, such as breast and colorectal cancers, which are closely related to unfavorable prognosis.[46] Targeting STAT3 has emerged as a promising therapeutic strategy for cancer therapy and is actively being developed.[47] The SH2 domain of STAT3, which contains three binding pockets (pY705, pY+1, and pY-X), is the critical targeting domain for current drug development.[48,49] However, the widespread expression of STAT3 in various cells makes the development of its target drugs face possible undesirable side effects, emphasizing the critical need for a comprehensive understanding of the precise mechanism of STAT3.[50,51] In this study, we identified the precise binding sequence between PALLD and STAT3, and designed a related peptide C-P3, which can impact the PALLD-STAT3 interaction, promoting the activation of STAT3. Therefore, our findings may offer more precise and efficacious targets for the design of STAT3-targeting drugs. In summary, our study revealed that the PALLD-STAT3 interaction plays a crucial role in regulating megakaryocyte differentiation. By targeting the binding site between PALLD and STAT3, we designed a peptide that effectively ameliorates thrombocytopenia in mice, providing new in-

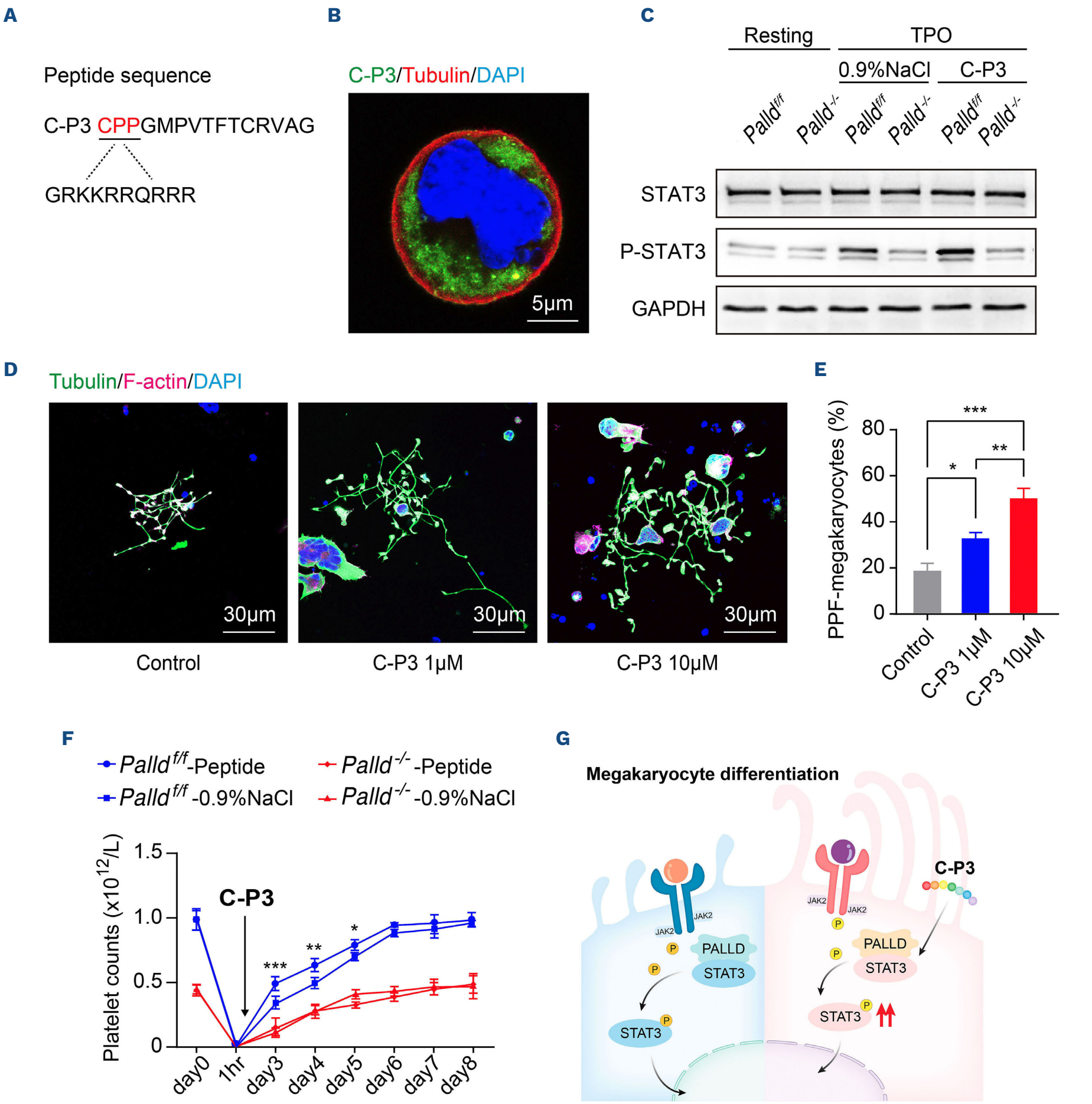

Figure 7. Peptide C-P3 promotes megakaryocyte differentiation and platelet production. (A) Sequences of peptide C-P3 fused to N-terminal cell-penetrating peptide (CPP). (B) Immunofluorescence (IF) images of α-tubulin (Rhodamine) in megakaryocytes treated with FITC-labeled C-P3. The scale bars represent 5 μm. (C) Western blot analysis of STAT3 phosphorylation level in *Palld*$^{f/f}$ and *Palld*$^{-/-}$ platelets incubated with 0.9% NaCl or C-P3. (D) IF images of fetal liver-derived megakaryocytes stimulated with phosphate-buffered saline (PBS) or 1 μM and 10 μM C-P3. Stained for α-tubulin (Alexa Fluor 488) and F-actin (Alexa Fluor 647). The scale bars represent 30 μm. (E) Quantitative analysis of the ratio of proplatelet-forming (PPF)-megakaryocytes to total megakaryocytes (N=6; **P*<0.05, ***P*<0.01, ****P*<0.001). (F) Platelets of *Palld*$^{f/f}$ and *Palld*$^{-/-}$ mice were eliminated by intravenous tail injection of anti-CD42b antibody (2 μg/g). After 36 hours, a bone marrow injection of C-P3 (20 μg/g) was performed. Platelet counts were measured at various time intervals (N=4; **P*<0.05, ***P*<0.01, ****P*<0.001). (G) Schematic diagram of peptide C-P3-induced enhancement of megakaryocyte differentiation.

sights and a potential target for the clinical treatment of thrombocytopenia.

Disclosures

No conflicts of interest to disclose.

Contributions

GL, YX, JL, HJ and XC designed the experiments, analyzed data, and wrote the paper. GL, YX and HJ performed the experiments. XC provided the animal model. LW, TL, CD, MY, MX, YS, LZ and JD helped with experiments.

Acknowledgments

The authors thank the technical support from the Core Facility of Basic Medical Sciences in Shanghai Jiao Tong University School of Medicine.

Funding

This work was supported by the National Natural Science Foundation of China (82322004, 82170126, 82030004, 31830050, 82200131 and 81970127), the National Key R&D Program of China (2021YFA0804900 and 2023YFC2507800), the Postdoctoral Fellowship Program of CPSF (GZB20230432), the Innovative research team of high-level local universities in Shanghai (SHSMU-ZDCX20211801), and the Bureau of Xiangyang City Science and Technology Project (2022YL02A).

Data-sharing statement

The data that support the findings of this study are available from the corresponding author Y. Xu upon reasonable request.

References

1. Stanworth SJ, Shah A. How I use platelet transfusions. Blood. 2022;140(18):1925-1936.
2. Corash L, Chen HY, Levin J, et al. Regulation of thrombopoiesis: effects of the degree of thrombocytopenia on megakaryocyte ploidy and platelet volume. Blood. 1987;70(1):177-185.
3. Thachil J, Warkentin TE. How do we approach thrombocytopenia in critically ill patients? Br J Haematol. 2017;177(1):27-38.
4. Machlus KR, Italiano JE Jr. The incredible journey: from megakaryocyte development to platelet formation. J Cell Biol. 2013;201(6):785-796.
5. Noetzli LJ, French SL, Machlus KR. New insights into the differentiation of megakaryocytes from hematopoietic progenitors. Arterioscler Thromb Vasc Biol. 2019;39(7):1288-1300.
6. Tilburg J, Becker IC, Italiano JE. Don't you forget about me(gakaryocytes). Blood. 2022;139(22):3245-3254.
7. Bluteau D, Lordier L, Di Stefano A, et al. Regulation of megakaryocyte maturation and platelet formation. J Thromb Haemost. 2009;7(Suppl 1):227-234.
8. Kaushansky K, Lok S, Holly RD, et al. Promotion of megakaryocyte progenitor expansion and differentiation by the c-Mpl ligand thrombopoietin. Nature. 1994;369(6481):568-571.
9. Drachman JG, Sabath DF, Fox NE, Kaushansky K. Thrombopoietin signal transduction in purified murine megakaryocytes. Blood. 1997;89(2):483-492.
10. Johnson DE, O'Keefe RA, Grandis JR. Targeting the IL-6/JAK/STAT3 signalling axis in cancer. Nat Rev Clin Oncol. 2018;15(4):234-248.
11. Kuter DJ. New thrombopoietic growth factors. Blood. 2007;109(11):4607-4616.
12. Gurney AL, Wong SC, Henzel WJ, de Sauvage FJ. Distinct regions of c-Mpl cytoplasmic domain are coupled to the JAK-STAT signal transduction pathway and Shc phosphorylation. Proc Natl Acad Sci U S A. 1995;92(12):5292-5296.
13. Sun L, Yan Y, Lv H, et al. Rapamycin targets STAT3 and impacts c-Myc to suppress tumor growth. Cell Chem Biol. 2022;29(3):373-385.
14. Tripathi SK, Chen Z, Larjo A, et al. Genome-wide analysis of STAT3-mediated transcription during early human Th17 cell differentiation. Cell Rep. 2017;19(9):1888-1901.
15. Goicoechea SM, Arneman D, Otey CA. The role of palladin in actin organization and cell motility. Eur J Cell Biol. 2008;87(8-9):517-525.
16. Parast MM, Otey CA. Characterization of palladin, a novel protein localized to stress fibers and cell adhesions. J Cell Biol. 2000;150(3):643-656.
17. Mykkänen OM, Grönholm M, Rönty M, et al. Characterization of human palladin, a microfilament-associated protein. Mol Biol Cell. 2001;12(10):3060-3073.
18. Jin L, Gan Q, Zieba BJ, et al. The actin associated protein palladin is important for the early smooth muscle cell differentiation. PLoS One. 2010;5(9):e12823.
19. Shu X, Chen M, Liu SY, et al. Palladin promotes cancer stem cell-like properties in lung cancer by activating Wnt/β-Catenin signaling. Cancer Med. 2023;12(4):4510-4520.
20. Chen X, Fan X, Tan J, et al. Palladin is involved in platelet activation and arterial thrombosis. Thromb Res. 2017;149:1-8.
21. Xu Y, Ouyang X, Yan L, et al. Sin1 (stress-activated protein kinase-interacting protein) regulates ischemia-induced microthrombosis through integrin αIIbβ3-mediated outside-in signaling and hypoxia responses in platelets. Arterioscler Thromb Vasc Biol. 2018;38(12):2793-2805.
22. Jiang H, Yu Z, Ding N, et al. The role of AGK in thrombocytopoiesis and possible therapeutic strategies. Blood. 2020;136(1):119-129.
23. Tiedt R, Schomber T, Hao-Shen H, Skoda RC. Pf4-Cre transgenic mice allow the generation of lineage-restricted gene knockouts for studying megakaryocyte and platelet function in vivo. Blood. 2007;109(4):1503-1506.
24. Skarnes WC, Rosen B, West AP, et al. A conditional knockout resource for the genome-wide study of mouse gene function. Nature. 2011;474(7351):337-342.
25. Kaushansky K. Thrombopoiesis. Semin Hematol. 2015;52(1):4-11.
26. Pang L, Xue HH, Szalai G, et al. Maturation stage-specific regulation of megakaryopoiesis by pointed-domain Ets proteins. Blood. 2006;108(7):2198-2206.
27. Vijey P, Posorske B, Machlus KR. In vitro culture of murine megakaryocytes from fetal liver-derived hematopoietic stem cells. Platelets. 2018;29(6):583-588.

28. Bush LM, Healy CP, Marvin JE, Deans TL. High-throughput enrichment and isolation of megakaryocyte progenitor cells from the mouse bone marrow. Sci Rep. 2021;11(1):8268.
29. Patel SR, Hartwig JH, Italiano JE Jr. The biogenesis of platelets from megakaryocyte proplatelets. J Clin Invest. 2005;115(12):3348-3354.
30. Yamamoto R, Morita Y, Ooehara J, et al. Clonal analysis unveils self-renewing lineage-restricted progenitors generated directly from hematopoietic stem cells. Cell. 2013;154(5):1112-1126.
31. Plo I, Bellanné-Chantelot C, Mosca M, et al. Genetic alterations of the thrombopoietin/MPL/JAK2 axis impacting megakaryopoiesis. Front Endocrinol (Lausanne). 2017;8:234.
32. Rachlin AS, Otey CA. Identification of palladin isoforms and characterization of an isoform-specific interaction between Lasp-1 and palladin. J Cell Sci. 2006;119(Pt 6):995-1004.
33. Wagstaff KM, Sivakumaran H, Heaton SM, Harrich D, Jans DA. Ivermectin is a specific inhibitor of importin α/β-mediated nuclear import able to inhibit replication of HIV-1 and dengue virus. Biochem J. 2012;443(3):851-856.
34. Fung HY, Chook YM. Atomic basis of CRM1-cargo recognition, release and inhibition. Semin Cancer Biol. 2014;27:52-61.
35. Jans DA, Martin AJ, Wagstaff KM. Inhibitors of nuclear transport. Curr Opin Cell Biol. 2019;58:50-60.
36. Kalderon D, Roberts BL, Richardson WD, Smith AE. A short amino acid sequence able to specify nuclear location. Cell. 1984;39(3 Pt 2):499-509.
37. Lu J, Wu T, Zhang B, et al. Types of nuclear localization signals and mechanisms of protein import into the nucleus. Cell Commun Signal. 2021;19(1):60.
38. Copolovici DM, Langel K, Eriste E, Langel Ü. Cell-penetrating peptides: design, synthesis, and applications. ACS Nano. 2014;8(3):1972-1994.
39. Albraiki S, Ajiboye O, Sargent R, Beck MR. Functional comparison of full-length palladin to isolated actin binding domain. Protein Sci. 2023;32(5):e4638.
40. Gilam A, Conde J, Weissglas-Volkov D, et al. Local microRNA delivery targets Palladin and prevents metastatic breast cancer. Nat Commun. 2016;7:12868.
41. Chin YR, Toker A. The actin-bundling protein palladin is an Akt1-specific substrate that regulates breast cancer cell migration. Mol Cell. 2010;38(3):333-344.
42. Wang W, Goswami S, Lapidus K, et al. Identification and testing of a gene expression signature of invasive carcinoma cells within primary mammary tumors. Cancer Res. 2004;64(23):8585-8594.
43. Liu H, Zhang Y, Li L, et al. Fascin actin-bundling protein 1 in human cancer: promising biomarker or therapeutic target? Mol Ther Oncolytics. 2021;20:240-264.
44. Mazzi S, Dessen P, Vieira M, et al. Dual role of EZH2 in megakaryocyte differentiation. Blood. 2021;138(17):1603-1614.
45. Hillmer EJ, Zhang H, Li HS, Watowich SS. STAT3 signaling in immunity. Cytokine Growth Factor Rev. 2016;31:1-15.
46. Yu H, Pardoll D, Jove R. STATs in cancer inflammation and immunity: a leading role for STAT3. Nat Rev Cancer. 2009;9(11):798-809.
47. Zou S, Tong Q, Liu B, et al. Targeting STAT3 in cancer immunotherapy. Mol Cancer. 2020;19(1):145.
48. Kraskouskaya D, Duodu E, Arpin CC, Gunning PT. Progress towards the development of SH2 domain inhibitors. Chem Soc Rev. 2013;42(8):3337-3370.
49. Furtek SL, Backos DS, Matheson CJ, Reigan P. Strategies and approaches of targeting STAT3 for cancer treatment. ACS Chem Biol. 2016;11(2):308-318.
50. Beebe JD, Liu JY, Zhang JT. Two decades of research in discovery of anticancer drugs targeting STAT3, how close are we? Pharmacol Ther. 2018;191:74-91.
51. Wong ALA, Hirpara JL, Pervaiz S, et al. Do STAT3 inhibitors have potential in the future for cancer therapy? Expert Opin Investig Drugs. 2017;26(8):883-887.